Impact Evaluation of Full-Span Slot and Blade-End Slot on Performance of a Large Camber Compressor Cascade

H. Wang, B. Liu†, B. Zhang and Z. Chen

School of Power and Energy, Northwestern Polytechnical University, Xi'an, Shaanxi, 710072, P. R. China

†*Corresponding Author Email: liubo704@nwpu.edu.cn*

ABSTRACT

It has been proved that suitable slot structure of compressor slotted blade can generate high-momentum jet flow through pressure difference between the pressure and suction surface, the slot jet flow can reenergize the local low-momentum fluid to effectively eliminate the flow separation. In order to investigate and evaluate the impact of full-span slot and blade-end slot on the performance of the post-loaded blade, which has serious flow separation on the suction surface both near blade midspan and endwall, a diffusion stator cascade with large camber angle is selected as the research object. Firstly, the blade-end slotted scheme and the full-span slotted scheme are set up. Then the performance of datum cascade and two slotted cascades is computed in the wide incidence angle range of -8º to 6º at the Mach number of 0.7, the corresponding blade-chord-based Reynolds number Re_C is 7.7×10^5. Finally, the performance of the three cascades is analyzed and compared. The results show that, in the computational incidence angle range, both of the two slotted schemes can reduce the total pressure loss for datum cascade and enhance its pressure diffusing capability. However, compared with the blade-end slot, the full-span slot has a better comprehensive control effect on the corner separation and the boundary layer separation near blade midspan, hence, compared with those of blade-end slotted cascade, the total pressure loss coefficients and the static pressure coefficients of full-span slotted cascade are respectively further decreased and increased. Under the blowing effect of full-span slot jet, the total pressure loss coefficients of datum cascade are significantly decreased, ranging as high as 21.2%, 23.1%, 24.5% and 23.4% under the incidence angles of 0°, 2°, 4° and 6°, respectively. The full-span slotted scheme has a better adaptability to wide incidence angle range, it can effectively broaden the available incidence angle range for datum cascade.

Keywords: Flow separation; Blade-end slot; Full-span slot; Post-loaded blade; Total pressure loss; Pressure diffusing capability.

NOMENCLATURE

C	chord length	$\overline{\omega}$	total pressure loss coefficient
H	blade height	P_{01}	inlet total pressure
t	blade pitch	P_{02}	local total pressure
β_S	stagger angle	Cp	static pressure coefficient
β_{1k}	geometric inlet angle	$\overline{\omega}_{cr}$	critical total pressure loss coefficient
β_{2k}	geometric outlet angle	$\overline{\omega}_{min}$	minimum total pressure loss coefficient
i	incidence angle	S1	plane perpendicular to the x axis
β_1	airflow inlet angle	TE	Trailing Edge
β_2	airflow outlet angle	x	spanwise direction
Ma_1	inlet Mach number	y	pitchwise direction
Re_C	blade-chord-based Reynolds number	z	axial direction
X	throat width of slot	P_1	inlet static pressure
R	lower surface radius of slot	P_2	local static pressure
LE	Leading Edge	PS	Pressure Surface
Ca	axial chord length	SS	Suction Surface
RANS	Reynolds Averaged Navier-Stokes	SA	Spalart-Allmaras

1. INTRODUCTION

As one of the core components of aeroengine, compressor has been developing mainly toward highly-loaded design direction in recent years (Eshraghi *et al.* 2016). Wennerstrom (1990) investigated and summarized the design methods that successfully increased the compressor load up to the 1970s**.** However, lots of highly loaded design methods failed, because of the ignorance of the generally accepted aerodynamic loading limit. The increase of load will intensify the flow separation inside compressor, resulting in an increase of total pressure loss and the narrowing of the available incidence angle range of compressor blade. Under this circumstance, when the incidence angle of incoming flow is large, large area of flow separation is prone to occur on the suction surface (SS) of compressor blade, which will make the compressor enter the stall and surge condition (Bright *et al.* 2005; Sanjay 2005). Besides, with the increase of compressor load, as an inherent flow feature in the blade-end region of compressor (Wisler 1985), three-dimensional corner separation may lead to the corner stall, thus contributing greatly to the passage blockage and loss. Therefore, three-dimensional corner separation is considered as one of the most important factors limiting the loading capacity of compressor (Zambonini 2017). Hence, for the increase of compressor blade load, it is necessary to use reasonable flow control methods to control the corner separation (Lord 2000).

Up to now, some flow control methods have shown certain potential in increasing compressor load. For example: boundary layer suction (Mao *et al.* 2018; Gbadebo *et al.* 2008), plasma excitation (Jothiprasad *et al.* 2012), end-bend blade (Kan *et al.* 2020) and slotted blade (Wu *et al.* 2013; Tang *et al.* 2019) etc. However, the first two methods belong to the active control methods and require complicated additional devices. Although their control effects on flow separation are better, they still have certain limitations in engineering applications. By contrast, slotted blade belongs to the passive control methods and has certain cost-effectiveness, so it has been studied by many scholars.

Zhou *et al.* (2009) performed slotted treatment on the stator blades of a single-stage compressor and found that due to the blowing effect of the slot jet, the pressure ratio and efficiency of the compressor have been improved, verifying the applicability of slotted blade in compressor. Ramzi and AbdErrahmane (2013) conducted two-dimensional computations on slotted cascades in stall condition and explored the impact of slot geometric parameters on the performance of slotted cascades. The results showed that the loss coefficient could be decreased by up to 28%, and the airflow turning angle could be increased up to 5°. Tang *et al.* (2018a) applied the slot structure to the blade end of a cascade with low aspect ratio, finding that when the slot outlet is set before the separation point, the slot jet has a better control effect on the corner separation. Additionally, Liu *et al.* (2016) studied the effects of cascade parameters such as consistency and aspect ratio on the performance of blade-end slotted cascades. The results showed that the application of the slot structure could effectively suppress the serious flow separation caused by the increase of load, which is beneficial to increase the aeroengine thrust-to-weight ratio by reducing blade number.

The above studies have verified the feasibility of effective control on flow separation through slot jet, however, there are relatively few studies on the performance evaluation of full-span slotted cascade and blade-end slotted cascade. The study of Tang *et al.* (2018b) found that for the front-loaded blade with severe corner separation and no separation near blade midspan, under most incidence angles of the computational incidence angle range, due to the mixing effect of the full-span slot jet and the main flow, the wake loss near blade midspan would be increased, resulting in the loss coefficients of full-span slotted cascade are larger than those of blade-end slotted cascade. Based on the study of Tang *et al.* (2018b), the aim of this study is to investigate the performance impact of the full-span slot and the blade-end slot on the post-loaded blade, which has severe flow separation both in the blade-end region and near blade midspan. First of all, a diffusion stator cascade with a large camber angle of 53.38° is selected as the research datum cascade, and the blade-end slot and the full-span slot are respectively applied to the datum cascade. Afterwards, the performance of datum cascade and two slotted cascades is computed in a wide incidence angle range at a constant Mach number. At last, the flow structures and aerodynamic parameters such as total pressure loss, airflow turning angle (Airflow inlet angle β_1 minus outlet angle β_2) and static pressure coefficient of the three cascades are analyzed and compared.

2. MODELS AND METHODS

2.1 Datum Cascade Model

A diffusion stator cascade with a large camber angle of 53.38° is selected as the research datum cascade in this study, its schematic is shown in Fig. 1. It can be found that the blade profile of datum cascade is a post-loaded blade profile, the middle arc camber of which is more concentrated on the second half of the blade.
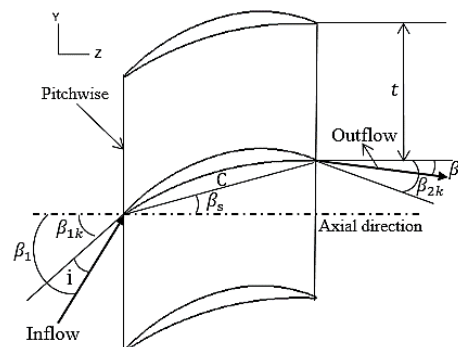

**Fig. 1. Two-dimensional datum cascade configuration**

Detailed geometric and aerodynamic parameters of datum cascade are shown in Table 1. When the Mach number Ma_1 of incoming flow is 0.7, in the available range of incidence angles, the flow separation on the SS of the cascade are serious both in the blade-end region and near blade midspan. Moreover, the blade-chord-based Reynolds number Re_C=7.7 × 10^5.

Table 1 Datum cascade parameters

parameters	values
Chord C/mm	63
Blade height H/mm	100
Aspect ratio H/C	1.59
Blade pitch t/mm	43.15
Blade solidity C/t	1.46
Stagger angle β_S/(°)	15.4
Geometric inlet angle β_{1k}/(°)	40.17
Geometric outlet angle β_{2k}/(°)	-13.21
Inlet Mach number Ma_1	0.7
Re_C	7.7×10^5

2.2 Slotted Cascade Models

The geometry of the slot configuration used in this study is shown in Fig. 2. Line AB and line CD respectively represent the slot upper and lower boundaries. The axial outlet position of the slot is selected as 70% of axial chord length (Ca), and the slot length is 0.4Ca. Furthermore, the inlet and outlet widths of the slot is 0.25Ca and 0.15Ca, respectively. The study of Liu *et al.* (2016) showed that the tangency between the slot upper wall and the blade pressure surface (PS) contributes to introducing the main flow of the blade pressure side into the slot without additional loss. Therefore, line AB is set to tangent to the blade PS at point A.
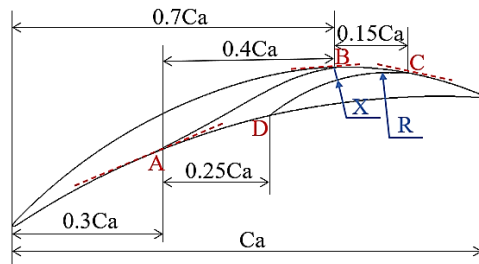

Fig. 2. Geometry of slot configuration.

In order to ensure that the slot jet direction is consistent with that of the main flow, line AB and line CD are respectively set to tangent to the blade SS at point B and point C, which can reduce the mixing loss between the slot jet and the main flow and enhance the blowing effect of slot jet on local low-momentum fluid (Denton 1993). As proved previously, due to the balance between the centrifugal force around the curved surface and the subambient pressure in the jet sheet, the Conada jet remains attached to curved surface (Jones *et al.* 2002). Hence, for the aim to ensure the slot jet flows along the outlet curved surface of the slot lower wall

without separation, the ratio X/R between the slot throat width (X) and the slot lower wall outlet curve radius (R) is kept at a small value of 0.04, which also further ensures the direction consistency of the slot jet and the main flow.

Based on the slot configuration shown in Fig. 2, the full-span slotted scheme and the blade-end slotted scheme are set up, the slot height of full-span slotted cascade occupies 100% of the blade span. The three-dimensional geometric model of blade-end slotted cascade is shown in Fig. 3, the axial outlet position of the blade-end slot is kept consistent with that of the full-span slot, which is 0.7Ca. Besides, in order to avoid that the mixing effect of the slot jet and the main flow increases the wake loss near blade midspan and to effectively suppress the corner separation (Tang *et al.* 2018b), the blade-end slot height is selected as 25% of blade height (H)
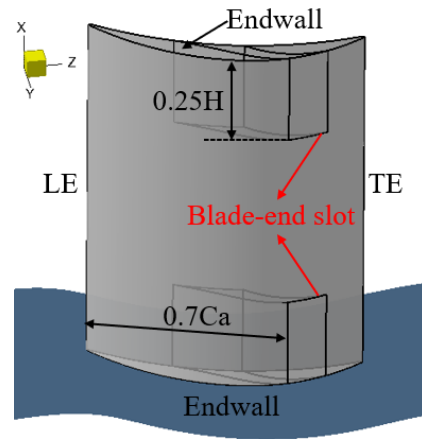

Fig. 3. Three-dimensional geometric model for blade-end slotted cascade

2.3 Numerical Method

In this study, a structured O4H mesh topology is automatically generated by AUTOGRID5 (2009) from NUMECA international for the cascade passage, the passage grid number of datum cascade is kept as same as that of slotted cascades, which contains 1.5 million grid points. For the slot, a structured H mesh topology is manually generated by IGG module (2009) of NUMECA International, the grid number of the full-span slot is 0.38 million. Afterwards, according to the ratio of the blade-end slot height to H, the total grid number of two blade-end slots of blade-end slotted cascade is selected as 0.19 million, and the grid distribution of the blade-end slot along pitchwise direction and axial direction is consistent with that of the full-span slot grid. In addition, a complete non-matching connection is adopted between the slot grid and the cascade passage grid, ensuring the validity of the numerical value transfer during computation, and both of the blade and the endwall are set to be non-slip adiabatic walls. Taking full-span slotted cascade as an example, its passage grid and slot grid are shown in Fig. 4, the periodic boundary condition is set on both sides of the flow passage, and the inlet and outlet planes are respectively located at 1.0C upstream of

the blade leading edge (LE) and 1.5C downstream of the blade trailing edge (TE). Additionally, the size and density of mesh near the blade and endwall surfaces were refined during the computational procedure so as to capture the boundary layer and near-endwall secondary flow, based on which, the 3D mesh can be obtained by non-uniformly duplicating the plane mesh along the spanwise direction into 181 planes (full span).
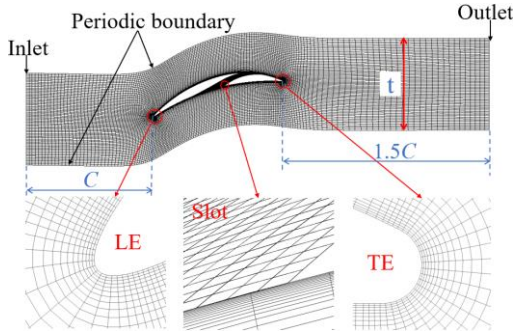

**Fig. 4. Computational grid for full-span slotted cascade.**

In this study, the inlet Mach number is selected as a constant value of 0.7. For the aim to evaluate the performance of datum cascade and two slotted cascades in the available incidence angle range, the inlet incidence angle range is selected as -8º to 6º (2º interval). Besides, the inlet total temperature and total pressure are respectively selected as 288.15K and 101325Pa. The studies of Cao *et al.* (2014, 2017) showed that the Spalart-Allmaras (SA) turbulence model could effectively Capture the details of the flow field of the cascade, which has the same blade profile with the datum cascade used in this study, hence the SA turbulence model is adopted in the numerical computational process. Due to the direction consistency of the slot jet flow and the main flow, the influence of the slot jet flow is limited to the single blade passage, therefore, one blade passage is simulated and computed. Afterwards, the three-dimensional Reynolds Averaged Navier-Stokes (RANS) simulations are conducted with FINE/Turbo (2009) from NUMECA International. In the computational process, the central difference format with second-order accuracy is adopted as the spatial discretization format, and both of the multi-grid acceleration technology and the implicit residual smoothing method are used to accelerate the computational convergence.

In order to eliminate the influence of grid number on the computational results, the grid independences of datum cascade and full-span slotted cascade are verified under the large separation condition. Figure 5(a) shows the spanwise distribution of pitch-averaged total pressure loss coefficients of datum cascade at outlet under 6º incidence angle. It can be seen that when the grid points exceed 1.5 million, the computational results of datum cascade tend to be converged. For full-span slotted cascade, the cascade passage grid number is kept unchanged as 1.5 million, Fig. 5(b) shows its spanwise distribution of

pitch-averaged total pressure loss coefficients at outlet under 6° incidence angle, the computational results show little difference when the slot grid number reaches 0.23 million. The definition of total pressure loss coefficient is shown in Eq. (1), where P_{01} and P_{02} respectively represent the inlet total pressure and the local total pressure, and P_1 represents the inlet static pressure. According to above analysis, the grid numbers of the cascade passage and the slot selected in this study can effectively ensure the validity of the computational results.
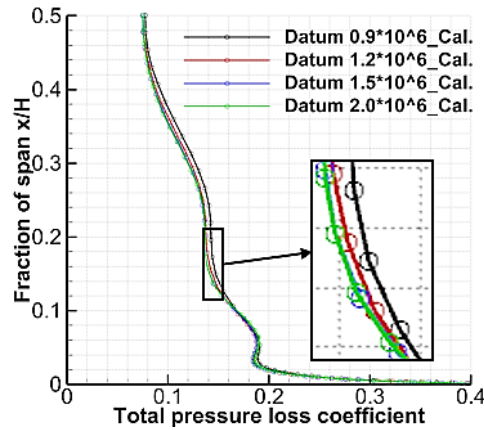

(a) Datum cascade
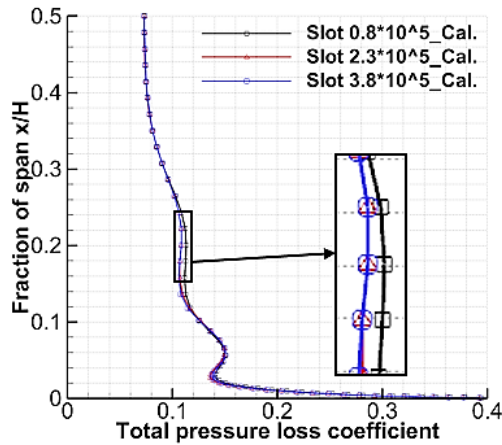
(b) Full-span slotted cascade

Fig. 5. Spanwise distribution of total pressure loss coefficients for different grid numbers under 6° incidence angle.

$$\overline{w} = \frac{P_{01} - P_{02}}{P_{01} - P_1} \tag{1}$$

$$c_P = \frac{P_2 - P_1}{P_{01} - P_1} \tag{2}$$

For the aim to further verify the reliability of the numerical method, the performance of datum cascade is computed at the Mach number of 0.6 when the blade solidity (C/t) is 1.66. Figure 6 compares the static pressure coefficients of the computational and experimental results at the midspan of datum cascade under 0.5° and 5° incidence angles, it can be found

that the numerical computational results are basically consistent with the experimental data, which proves that the numerical method adopted in this paper is reliable. The definition of static pressure coefficient is shown in Eq. (2), where P_2 represents the local static pressure, P_{01} and P_1 are consistent with the definition in Eq. (1).

(a) 0.5°

(b) 5°
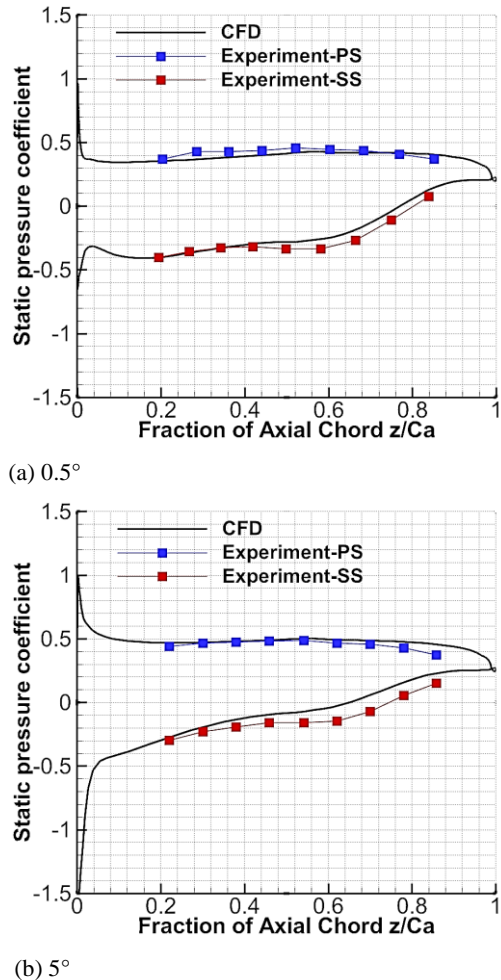
Fig. 6. Comparation between the computational results and experimental results under the incidence angles of 0.5° and 5.

RESULTS AND DISCUSSION

3.1 Performance Analysis under the Incidence Angle of 0°

Since the flow structure of linear stator cascade is symmetrical about the 50%H plane of the blade, to highlight the details of the flow field, the performance of datum cascade and two slotted cascades is analyzed within 0-50%H in this study. Figure 7 shows the volume streamlines in flow passage and static pressure contours on cutting plane for datum cascade and two slotted cascades under 0° incidence angle, the blue streamlines and red streamlines represent the main flow and the endwall secondary flow (The flow migrating from endwall to

SS), respectively, and the green streamlines represent the slot jet flow.

Due to the pressure gradient in the counter-streamwise direction, the endwall boundary layer and the SS boundary layer of datum cascade develop rapidly, and under the effect of mutual interference, they separate in the blade-end region, forming corner separation. And due to the passage blockage in the blade-end region and the pitchwise pressure gradient, the endwall secondary flow also migrates toward midspan on the SS of datum cascade and basically develops to 30%H. Furthermore, near blade midspan, the main flow also separates on the SS before reaching the TE. The boundary layer separation near blade midspan and the corner separation of datum cascade are both serious. For blade-end slotted cascade, its blade-end slot jet effectively suppresses the development of the endwall secondary flow on the SS, and the corner separation is basically eliminated, enhancing the flow capability in the blade-end region. However, the flow separation degree near blade midspan of blade-end slotted cascade is larger than that of datum cascade. For full-span slotted cascade, the midspan boundary layer separation and the corner separation are both effectively suppressed, due to the blowing effect of the full-span slot jet.

By observing the static pressure contours on cutting plane of the three cascades, it can be found that both of the two slotted schemes can enhance the pressure diffusing capability for datum cascade. But due to the flow separation near blade midspan, blade-end slotted cascade has smaller static pressure than full-span slotted cascade. Additionally, for blade-end slotted cascade, it can be seen that there exists a pressure difference between the blade-end region and the blade midspan, which causes the separated main flow above the slot to migrate toward midspan, intensifying the separation of the main flow near blade midspan.

Figure 8 shows the streamlines and total pressure loss in the S1 stream surfaces corresponding to 50%H and 10%H for three cascades under the incidence angle of 0°. It can be found that consistent with the analysis to Fig. 7, the flow separation degree of blade-end slotted cascade is larger than that of datum cascade at blade midspan, which leads to larger total pressure loss around TE. In contrast, the full-span slot jet effectively eliminates the separation and decreases the total pressure loss around TE. In the S1 stream surface corresponding to 10%H, the separation scope and the loss extent of datum cascade are large, but both of the blade-end slot jet and the full-span slot jet can effectively eliminate the separation and decrease the loss around TE, which makes the flow structures in the blade-end region of the two slotted cascades are better than that of datum cascade.

In order to further analyze the impact of the blade-slot jet and the full-span slot jet on the wake loss, Figure 9 shows the total pressure loss contours on the plane located 50%C downstream of TE for the three cascades under 0° incidence angle. It can be seen that due to the mixing effect of the full-span slot jet and

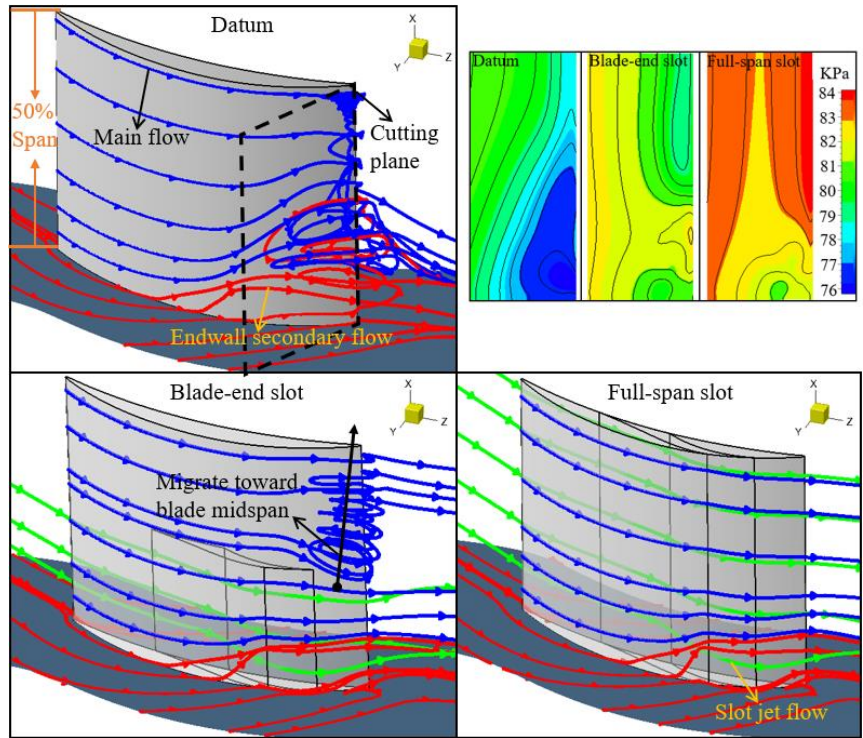**Fig. 7. Volume streamlines in flow passage and static pressure contours on cutting plane for datum cascade and two slotted cascades under 0° incidence angle.**
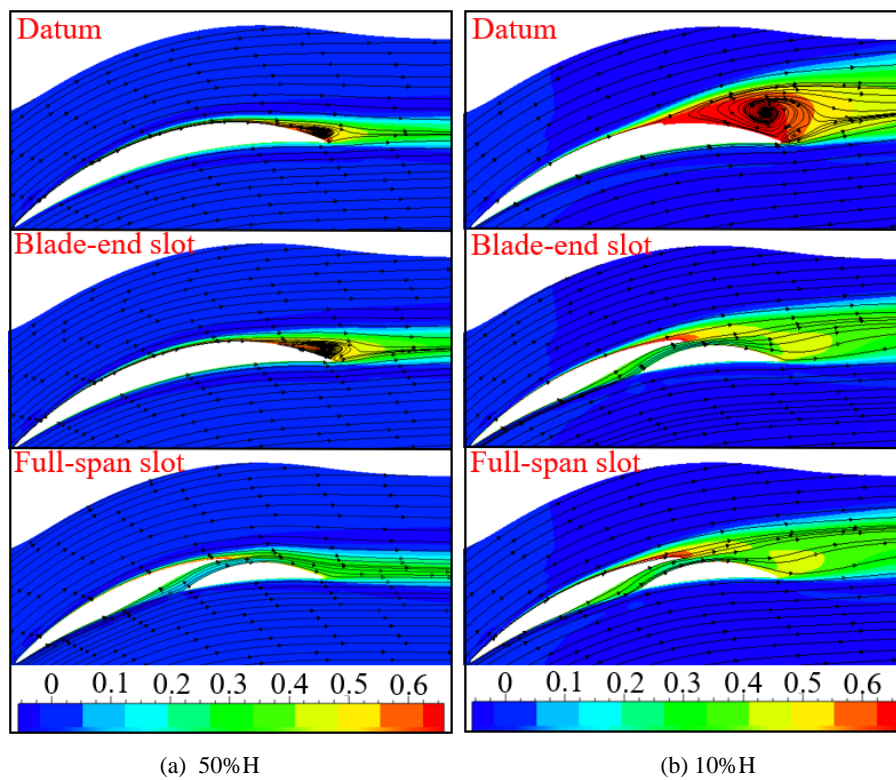

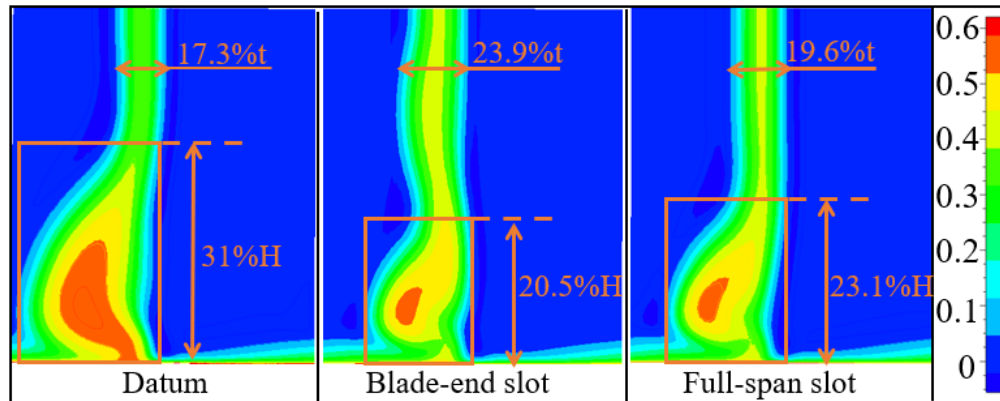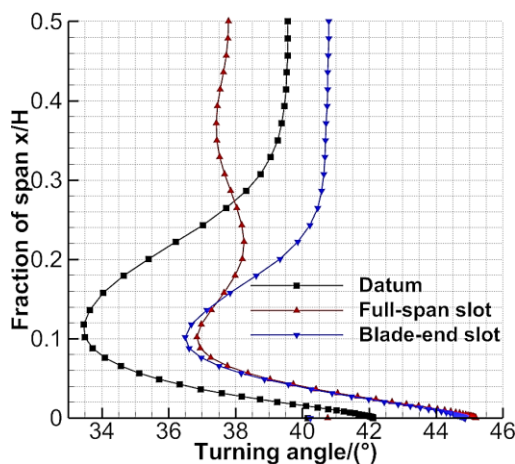(a) 50%H   (b) 10%H

Fig. 8. Streamlines and total pressure loss in the S1 stream surface for datum cascade and two slotted cascades under 0° incidence angle.

Fig.9. Total pressure loss contours for datum cascade and two slotted cascades under 0° incidence angle.

Fig. 10. Spanwise distribution of turning angles for datum cascade and two slotted cascades under 0° incidence angle.

the main flow, the extent and scope of the loss near blade midspan of full-span slotted cascade is larger than those of datum cascade, which is consistent with the conclusion of Tang *et al.* (2018b). But the loss of blade-end slotted cascade is larger compared with that of full-span slotted cascade near blade midspan, because the separated main flow above the blade-end slot migrates toward midspan, intensifying the flow separation near blade midspan.

In addition, in the blade-end region, the scope and extent of the loss of blade-end slotted cascade andfull-span slotted cascade are smaller than that of datum cascade, which is caused by the effective control effect of the blade-end slot jet and the full-span slot jet on the corner separation. Compared with that of full-span slotted cascade, the loss scope near endwall of blade-end slotted cascade is smaller, the reason is as follows: the boundary layer separation near blade midspan of blade-end slotted cascade leads to certain midspan passage blockage, which makes that the flow capability of the cascade is concentrated in the blade-end region, enhancing the control effect of the blade-end slot jet on the corner separation.

To evaluate the impact of the blade-end slot and the full-span slot on the turning angles of datum cascade, Figure 10 shows the spanwise distribution of pitch-averaged turning angles of the three cascades on the plane located 50%C downstream of the TE under 0° incidence angle. According to above analyses, near blade midspan, although the wake loss of full-span slotted cascade is increased compared with that of datum cascade as a result of the mixing effect of the full-span slot jet and the main flow, the boundary layer separation on the SS is eliminated, therefore, the airflow turning angles of full-span slotted cascade are larger than those of datum cascade. In contrast, the turning angles near blade midspan of blade-end slotted cascade are smaller than those of datum cascade, due to its large degree of the midspan boundary layer separation. However, in the blade-end region, the turning angles of the two slotted cascades are larger than those of datum cascade. Full-span slotted cascade has larger turning angles than blade-end slotted cascade almost within whole span, while the turning angles of blade-end slotted cascade are slightly larger in the 0-14%H interval, because the midspan passage blockage caused by relatively large separation enhances the flow capability in the blade-end region, which enhances the control effect of the blade-end slot jet on the corner separation.

3.2 Performance Analysis under the incidence angle of 6°

Figure 11 shows the volume streamlines in flow passage and static pressure contours on cutting plane for the three cascades under 6° incidence angle. It can be found that due to the large incidence angle, the airflow separates directly at the LE of datum cascade, afterwards, the separated airflow gradually adheres to the SS under the action of the main flow, forming a reattached line. Compared with the situation under 0° incidence angle, the corner separation scope of datum cascade under 6° incidence angle is further enlarged, and the endwall secondary flow basically migrates to blade midspan on the SS. Under the incidence angle of 6°, the corner separation of datum cascade leads to serious passage blockage, the flow capability of datum cascade is weak.
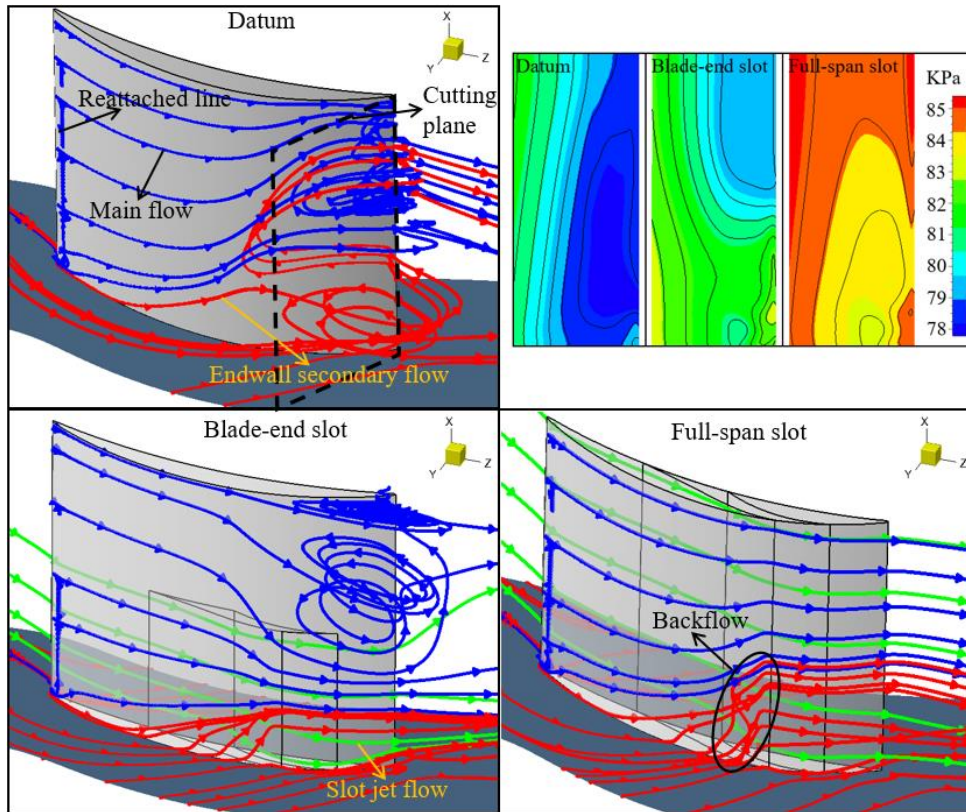
Fig. 11. Volume streamlines in flow passage and static pressure contours on cutting plane for datum cascade and two slotted cascades under 6° incidence angle.

Consistent with the situation under 0° incidence angle, both of the two slotted schemes can enhance the pressure diffusing capability. For blade-end slotted cascade, its blade-end slot jet basically eliminates the corner separation, enhancing the flow capability in the blade-end region. But due to the pressure difference between the blade-end region and the blade midspan, the separated main flow above the blade-end slot develops toward blade midspan, which intensifies the flow separation near blade midspan, contributing to serious midspan passage blockage. However, there nearly not exists flow separation on the SS within whole span for full-span slotted cascade, due to the blowing effect of the full-span slot jet. But its development scope of the secondary flow is larger than that of blade-end slotted cascade, and a small area of backflow (The flow in counter-axial direction) is formed near endwall before the full-span slot. The reason is as follows: The midspan passage blockage of blade-end slotted cascade enhances the flow capability in the blade-end region, which leads to better control effect of the blade-end slot jet on the secondary flow development and corner separation.

Figure 12 shows the streamlines and total pressure loss in the S1 stream surfaces corresponding to 50%H and 10%H for the three cascades under the incidence angle of 6°. It can be found that for datum cascade, compared with the situation under 0° incidence angle, the flow separation degree and the loss near TE are both larger at 50%H and 10%H under 6° incidence angle. Consistent with the

diagram of volume streamlines, at the blade midspan, blade-end slotted cascade has larger flow separation degree and total pressure loss than datum cascade, while those of full-span slotted cascade are smaller, since the full-span slot jet effectively eliminates the separation around TE. At 10%H, both of the blade-end slot jet and the full-span slot jet can basically suppress the flow separation and eliminate the separation around TE, but a small area of backflow exists before the full-span slot, which corresponds to the backflow zone on the SS of full-span slotted cascade in Fig. 11.

Figure 13 shows the total pressure loss contours on the plane located 50%C downstream of TE for the three cascades under 6° incidence angle. It can be found that for datum cascade, the influencing zone of the corner separation almost reaches blade midspan, the scope and extent of the loss near blade midspan and endwall are both large. However, due the effective suppressing effect of the blade-end slot jet on the corner separation, the loss near endwall of blade-end slotted cascade is smaller than that of datum cascade, but its loss near blade midspan caused by serious flow separation is greatly enlarged compared with that of datum cascade. For full-span slotted cascade, different form the situation under 0° incidence angle, the scope and extent of the loss near blade midspan are decreased compared with those of datum cascade, because the mixing loss of the slot jet and the main flow is smaller than the loss reduced by eliminating the separation. In addition, in the blade-end region, the loss of full-span slotted cascade is

(a) 50%H

(b)10%H
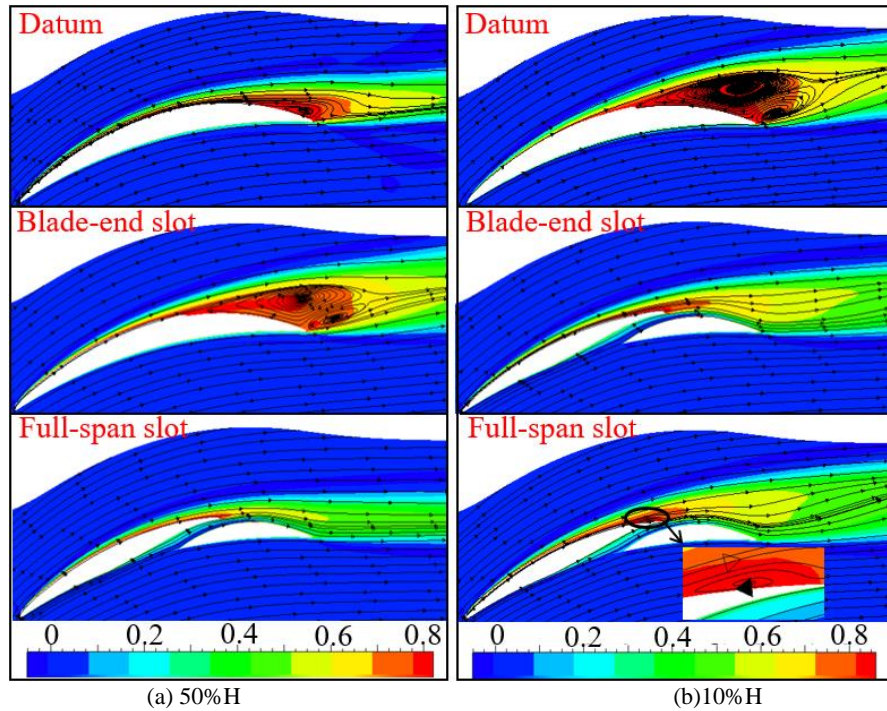
Fig. 12. Streamlines and total pressure loss in the S1 stream surface for datum cascade and two slotted cascades under 6° incidence angle.
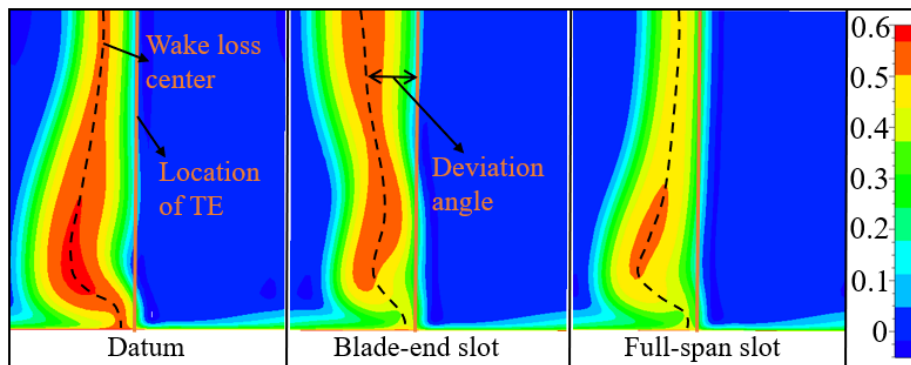
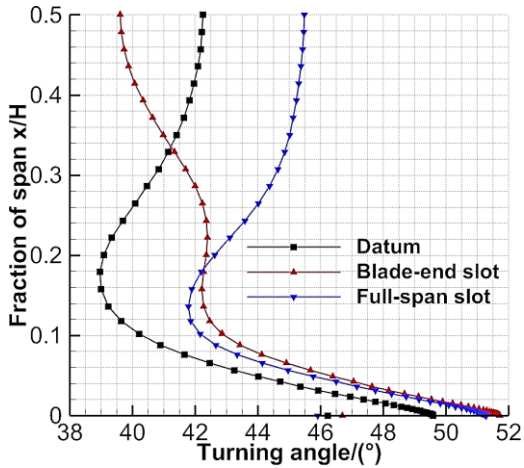**Fig. 13. Total pressure loss contours for datum cascade and two slotted cascades under 6° incidence angle.**

smaller than that of datum cascade and slightly larger than that of blade-end slotted cascade. Since the flow capability near endwall of blade-end slotted cascade is better than that of full-span slotted cascade, enhancing the suppressing effect of the blade-end slot jet on the corner separation.

By observing the wake loss centers of the three cascades, it can be found that near blade midspan, the loss center of blade-end slotted cascade is further away from TE compared with that of datum cascade, while the loss center of full-slotted slotted cascade is closer to TE. That is, the deviation angles near blade midspan of blade-end slotted cascade are larger than those of datum cascade, but full-span slotted cascade has smaller deviation angles near blade midspan than datum cascade. Because that the flow separation degree near blade midspan of blade-end slotted cascade is larger than that of datum cascade, while full-span slotted cascade has no flow separation on

the SS near blade midspan. Furthermore, in the blade-end region, the deviation angles of the two slotted cascades are smaller compared with those of datum cascade. But the midspan passage blockage of blade-end slotted cascade enhancing the control effect of the blade-end slot jet on the corner separation, leading to that blade-end slotted cascade has smaller deviation angles in the blade-end region than full-span slotted cascade.

For the aim to further evaluate the impact of the blade-end slot and the full-span slot on the turning angles of datum cascade, Fig. 14 shows the spanwise distribution of pitch-averaged turning angles of the three cascades on the plane located 50%C downstream of TE under 6° incidence angle. Consistent with the analyses to wake loss centers of the three cascades, compared with those of datum cascade, the turning angles near blade midspan of blade-end slotted cascade are smaller, while those of

Fig. 14. Spanwise distribution of turning angles for datum cascade and two slotted cascades under 6° incidence angle.

full-span slotted cascade are larger. Besides, in the blade-end region, both of blade-end slotted cascade and full-span slotted cascade have larger turning angles than datum cascade, due to the effective control effects of the blade-end slot jet and the full-span slot jet on the corner separation. However, the turning angles near endwall of blade-end slotted cascade are slightly larger than those of full-span slotted cascade, which is consistent with the situation under 0° incidence angle.

By combining the performance analyses for datum cascade and the two slotted cascades under the incidence angles of 0° and 6°, it can be found that under the two incidence angles, for the post-loaded blade with serious flow separation both near endwall and blade midspan, the blade-end slot jet and the full-span slot jet can effectively suppress the corner separation and decrease the wake loss in the blade-end region, enhancing the pressure diffusing capability of datum cascade. Near blade midspan, due to the mixing effect of the full-span slot jet and the main flow, the wake loss of full-span slotted cascade is slightly larger than that of datum cascade under 0° incidence angle, but the wake loss of blade-end slotted cascade is still larger than that of full-span slotted cascade, because the separated main flow above the blade-end slot migrates toward blade midspan, intensifying the boundary layer separation near blade midspan. Therefore, under the two incidence angles, due to the serious midspan flow separation of blade-end slotted cascade, its turning angles near blade-midspan are smaller than those of datum cascade, that is, the pressure diffusing capability near blade midspan of blade-end slotted cascade is weaker than that of datum cascade. However, the midspan passage blockage of blade-end slotted cascade enhances its flow capability in the blade-end region, which leads to better control effect of the blade-end slot jet on the corner separation, hence, the wake loss near endwall of blade-end slotted cascade is smaller than that of full-span slotted cascade, besides, blade-end slotted cascade also has larger turning angles near endwall.

3.3 Performance Analysis at wide incidence angle range

Due to the variable working conditions of aeroengine, compressor blades don't work only under a certain incidence angle, it is necessary to perform performance analysis and evaluation on datum cascade and the two slotted cascades in the available range of incidence angles. Figure 15 shows the incidence angle characteristics of the three cascades in the incidence angle range of -8° to 6°, it can be found that within the available range of incidence angles, both of the two slotted schemes can reduce the total pressure loss for datum cascade.

According to the analyses in section 3.2 and 3.3, due to the serious midspan flow separation on the SS of blade-end slotted cascade, its total pressure loss coefficients are larger than those of full-span slotted cascade under the incidence angles of 0° and 6°. However, different from the research conclusions for the front-loaded blade (Tang *et al.* 2018b), for the post-loaded blade with serious flow separation both near blade midspan and endwall, the total pressure loss coefficients of full-span slotted cascade are smaller than those of blade-end slotted cascade in the available incidence angle range. And the difference between the loss coefficients of the two slotted cascades gradually increases as incidence angle increases, due to that the midspan flow separation degree of blade-end slotted cascade becomes greater with the increase of incidence angle, while the full-span slot jet can eliminate the midspan flow separation in the full incidence angle range. Additionally, the difference of the loss coefficients between full-span slotted cascade and datum cascade also becomes larger as incidence angle increases, it can be summarized that the control effect of the full-span slot jet on the flow separation gets better with the increase of incidence angle.
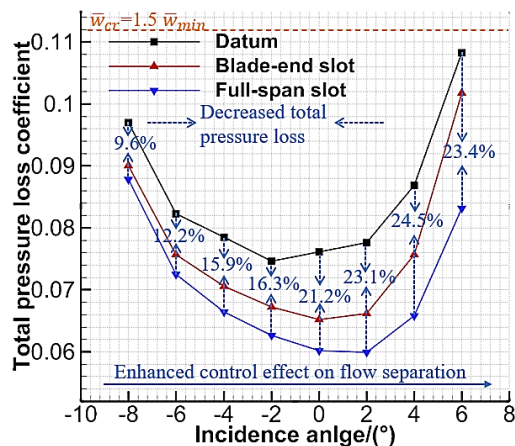
Fig. 15. Total pressure loss coefficients in the available incidence angle range for datum cascade and two slotted cascades.

Figure 16 shows the static pressure coefficients of the three cascades in the available range of incidence angles. In the available incidence angle range, the static pressure coefficients of the two slotted

cascades are larger than those of datum cascade, and full-span slotted cascade has slightly larger static pressure coefficients than blade-end slotted cascade, which is consistent with the analyses to turning angles. Furthermore, as incidence angle increases, the difference of the static pressure coefficients between the two slotted cascades gradually gets larger, due to the gradual serious midspan flow separation on the SS of blade-end slotted cascade, while the flow separation near blade midspan of full-span slotted cascade is eliminated in the full incidence angle range. Therefore, by observing the static pressure coefficients of the three slotted cascades under the incidence angles of 4° and 6°, it can be found that from 4° incidence angle to 6° incidence angle, the static pressure coefficient of datum cascade remains the same, and the static pressure coefficient of full-span slotted cascade increases, while that of blade-end slotted cascade decreases. That is, from 4° incidence angle to 6° incidence angle, the pressure diffusing capability of datum cascade is unchanged, and full-span slotted cascade has the enhanced pressure diffusing capability, while that of blade-end slotted cascade decreases. According to above analyses, the blade-end slotted scheme is not adaptable to the condition of large positive incidence angles, while full-span slotted scheme has a better adaptability to wide range of incidence angles.
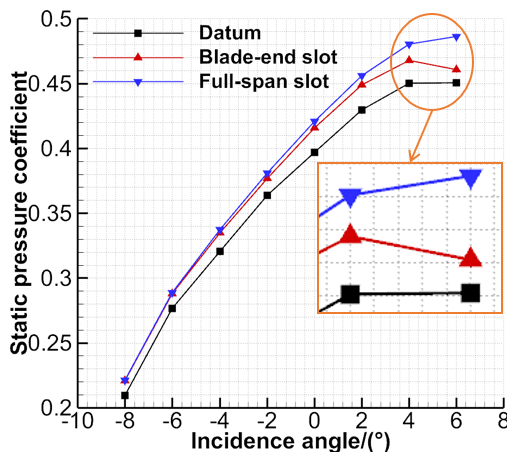
Fig. 16. Static pressure coefficients in the available incidence angle range for datum cascade and two slotted cascades.

4. CONCLUSION

A diffusion stator cascade with large camber angle is selected as the research object in this study, and the application of the full-span slot and the blade-end slot on the cascade has been investigated numerically in the wide incidence angle range of -8° to 6° at the Mach number of 0.7, the following main conclusions can be obtained:

(1) The full-span slot jet can effectively eliminate the boundary layer separation near blade midspan on the SS under the incidence angles of 0° and 6°. When the midspan flow separation of datum cascade is relatively weak (under 0° incidence angle), the mixing effect of the full-span slot jet and the main flow will enlarge the midspan wake loss. In contrast, when the midspan flow separation of datum cascade is serious (under 6° incidence angle), the midspan wake loss of full-span slotted cascade is smaller than that of datum cascade, because the mixing loss of the slot jet and the main flow is smaller than the loss reduced by eliminating the separation.

(2) Both of the blade-end slot jet and the full-span slot jet can effectively suppress the corner separation, but the improvement of the flow field in the blade-end region of blade-end slotted cascade leads to a pressure difference between the endwall and the blade midspan. Under the action of the pressure difference, the separated main flow above the blade-end slot migrates toward midspan, intensifying the separation of the main flow near blade midspan. Under the incidence angles of 0° and 6°, blade-end slotted cascade has larger wake loss and smaller turning angles than datum cascade near blade midspan, while the turning angles near blade midspan of full-span slotted cascade are larger than those of datum cascade. Besides, blade-end slotted cascade has slightly smaller wake loss and larger turning angles than full-span slotted cascade in the blade-end region, because the passage blockage near blade midspan caused by serious flow separation enhances the flow capability near endwall, which enhances the control effect of the blade-end slot jet on the corner separation.

(3) In the wide incidence angle range of -8° to 6°, the total pressure loss of the two slotted cascades are smaller than that of datum cascade, and their static pressure coefficients are larger, too. However, full-span slotted cascade has smaller total pressure loss and larger static pressure coefficients than blade-end slotted cascade, which means that for the post-loaded blade with serious flow separation both near blade midspan and endwall, the full-span slotted scheme has a better comprehensive control effect on the corner separation and midspan flow separation. Under the blowing effect of full-span slot jet, the total pressure loss coefficients of datum cascade are significantly decreased, ranging as high as 21.2%, 23.1%, 24.5% and 23.4% under the incidence angles of 0°, 2°, 4° and 6°, respectively. It can be summarized that full-span slotted scheme has a better adaptability to wide incidence angle range, it can effectively reduce the total pressure loss and enhance the pressure diffusing capability for datum cascade.

REFERENCES

AutoGrid5 v8.7, User Manual (2009). Brussels: NUMECA International.

Bright, M. M., D. E. Culley and E. P. Braunscheidel (2005). Closed Loop Active Flow Separation Detection and Control in a Multistage Compressor. *AIAA Paper,* 2005-0849.

Bright, Z., B. Liu and T. Zhang (2014). Control of separations in a highly loaded diffusion cascade by tailored boundary layer suction. *Proceedings of the Institution of Mechanical Engineers, Part C: Journal of Mechanical Engineering Science* 228(8), 1363–1374.

Cao, Z., B. Liu, T. Zhang, X. Yang and P. Chen (2014). Influence of coupled boundary layer suction and bowed blade on flow field and performance of a diffusion cascade. *Chinese Journal of Aeronautics* 30(1), 249–263.

Denton, J. D. (1993). Loss Mechanisms in Turbomachines. *Journal of Turbomachinery* 115(4), 621–656.

Eshraghi, H., M. Boroomand and A. M. Tousi (2016). A Developed Methodology in Design of Highly Loaded Tandem Axial Flow Compressor Stage. *Journal of Applied Fluid Mechanics* 9(1), 83-94.

FINE/Turbo v8.7, User Manual (2009). *Brussels: NUMECA International.*

Gbadebo, S. A., N. A. Cumpsty and T. P. Hynes (2008). Control of Three-Dimensional Separations in Axial Compressors by Tailored Boundary Layer Suction. *Journal of Turbomachinery* 130(1), 011004.

IGG v8.7, User Manual (2009). Brussels: NUMECA International.

Jones, G. S., A. E. Viken, L. N. Washburn, L. N. Jenkins and C. M. Cagle (2002). An Active Flow Circulation Controlled Flap Concept for General Aviation Aircraft Applications. *AIAA Paper* 2002-3157.

Jothiprasad, G., R. C. Murray, K. Essenhigh, G. A. Bennett, S. Saddoughi, A. Wadia and A. Breeze-Stringfellow (2012). Control of Tip-Clearance Flow in a Low Speed Axial Compressor Rotor with Plasma Actuation. *Journal of Turbomachinery* 134(2), 021019.

Kan, X., W. Wu and J. Zhong (2020). Effects of Vortex Dynamics Mechanism of Blade-End Treatment on the Flow Losses in a Compressor Cascade at Critical Condition. *Aerospace Science and Technology* 102(7), 105857.

Liu, Y., J. Sun, Y. Tang and L. Lu (2016). Effect of Slot at Blade Root on Compressor Cascade Performance Under Different Aerodynamic Parameters. *Applied Sciences* 6(12), 421.

Lord, W. K., D. G. Mac Martin and T. G. Tillman (2000). Flow control Opportunities in Gas Turbine Engines. *AIAA* 2000-2234.

Mao, X., B. Liu and T. Tang (2018). Control of Tip Leakage Flow in Axial Flow Compressor Cascade by Suction on the Blade Tip. *Journal of Applied Fluid Mechanics* 11(1), 137-149.

Ramzi, M. and G. AbdErrahmane (2013). Passive Control via Slotted Blading in a Compressor Cascade. *Journal of Applied Fluid Mechanics* 6(4), 571–580.

Sanjay, G. (2005). NASA Glenn Research in Controls and Diagnostics for Intelligent Aerospace Propulsion Systems. *NASA TM-2005-214036.*

Tang, Y., Y. Liu and L. Lu (2018b). Evaluation of Compressor Blading with Blade End Slots and Full-Span Slots in a Highly Loaded Compressor Cascade. *Journal of Turbomachinery* 141(12), 121002.

Tang, Y., Y. Liu and L. Lu (2018a). Solidity effect on corner separation and its control in a high-speed low aspect ratio compressor cascade. *International Journal of Mechanical Sciences* 142-143, 304–321.

Tang, Y., Y. Liu and L. Lu (2019). Passive Separation Control with Blade-End Slots in a Highly Loaded Compressor Cascade. *AIAA Journal* 58(1), 85-97.

Wennerstrom, A. J. (1990). Highly Loaded Axial Flow Compressors: History and Current Developments. *Journal of Turbomachinery* 112(4), 567-578.

Wisler, D. C. (1985). *Loss Reduction in Axial-Flow Compressors Through Low-Speed Model Testing. Journal of Engineering for Gas Turbines and Power* 107(2), 354.

Wu, P., R. Wang, K. Luo and F. Guo (2013). Effect of Slotted blade on Performance of High-Turning Angle compressor cascades. *Journal of Aerospace Power* 28(11), 2503-2509.

Zambonini, G., X. Ottavy and J. Kriegseis (2017). Corner Separation Dynamics in a Linear Compressor Cascade. *Journal of Fluids Engineering* 139(6), 061101.

Zhou, M., R. Wang, Y. Bai and L. Zeng (2009). Numerical Research on Effect of Stator Blade Slot Treatment on Single Stage Compressor Characteristic. *Acta Aerodynamica Sinica* 27(1), 114-118.